Interpretation of Specular XPCS measurements of Smectic Liquid Crystal Membranes

Irakli Sikharulidze*, Wim H. de Jeu

FOM-Institute for Atomic and Molecular Physics (AMOLF)

Amsterdam, The Netherlands

Anders Madsen	ID10, ESRF
Igor Dolbnya	B16, Diamond
Bela Farago	ILL
Andera Fera	AMOLF
Boris Ostrovskii	ICRAN, AMOLF

*) present address: Department of Biophysical Structural Chemistry (BFSC)

Leiden Institute of Chemistry

Leiden University, The Netherlands

Contents

- Smectic Liquid Crystal Membranes
  - Low-dimensional systems
  - Preparation
  - Relaxations of fluctuations
- X-ray Photon Correlation Spectroscopy (XPCS)
  - Experimental description
  - Results and Discussions

Smectic liquid crystal membranes

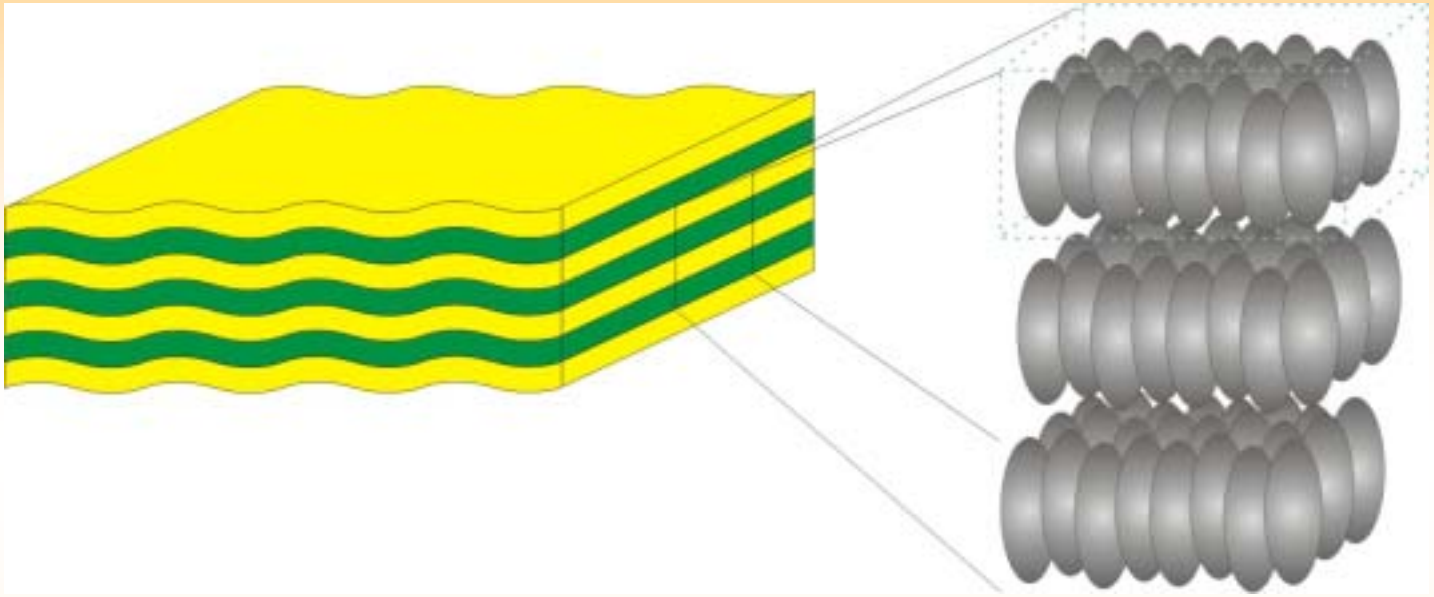

- Orientationally ordered elongated molecules
  (here assumed to be perfectly oriented).

- Stacked liquid layers give 1D ordering (smectic-A).

Properties of Smectic Membranes

- Very well oriented (mosaic < 1 up to 10 mdeg)
- Centro-symmetric (No substrate)
- From two to thousands of layers (about 5 nm to 20 μm)
- Cross-over from bulk behaviour (3D) in thick films to surface-dominated behaviour
- Model systems of low-dimensional ordering

W.H. de Jeu, B.I. Ostrovskii, A.N. Shalaginov, *Rev. Mod. Phys*. **75**, 181 (2003)

AMOLF FOM ESRF ILL NEUTRONS FOR SCIENCE

Smectic Liquid Crystal Molecules

K 33 CrB 48.5 SmA 63.5 N 73 I

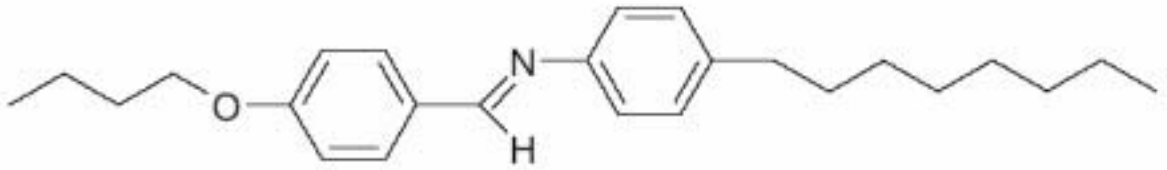

4O.8

K 72 SmC 79 SmA 129 I

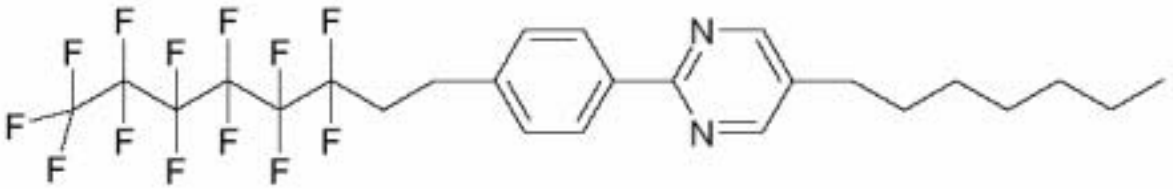

FPP

K 21.5 SmA 33.5 N 40.5 I

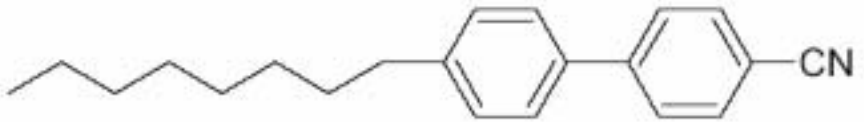

8CB

Preparation

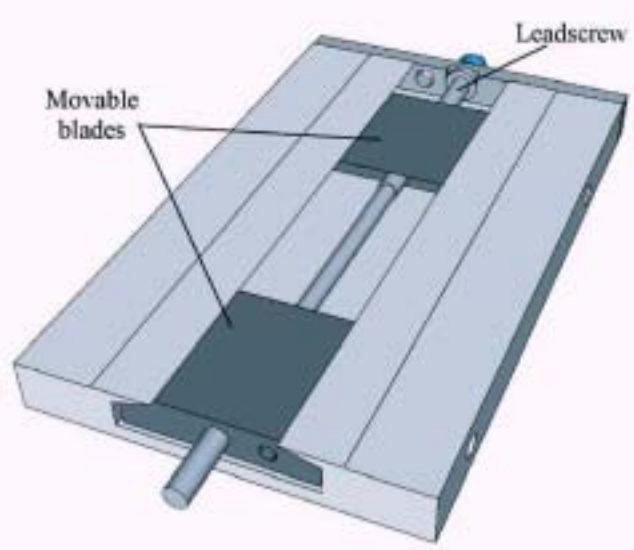

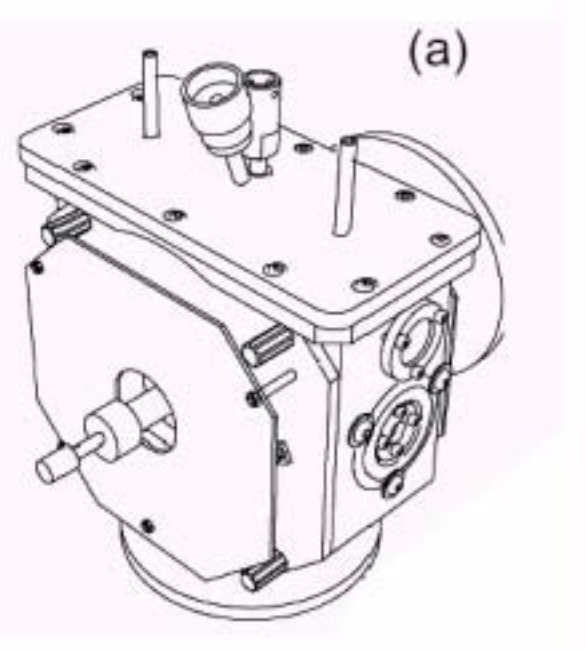

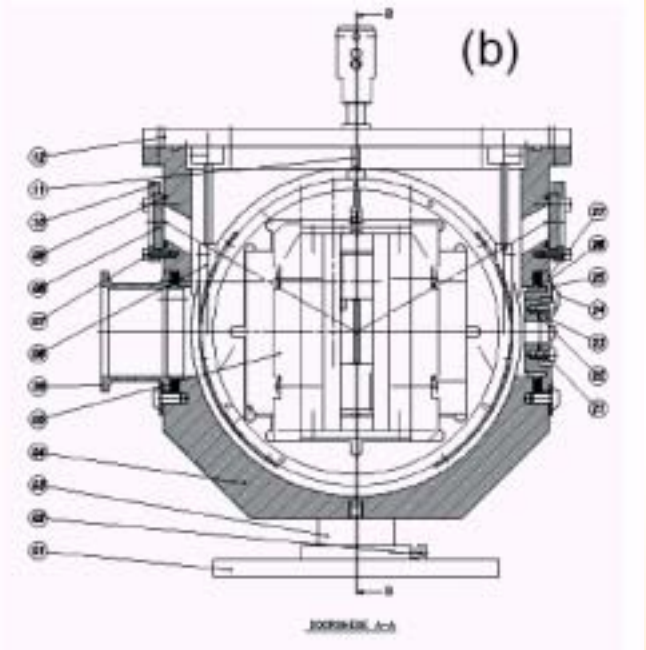

Typical sizes up to 25 × 70 mm^2

Reflectivity

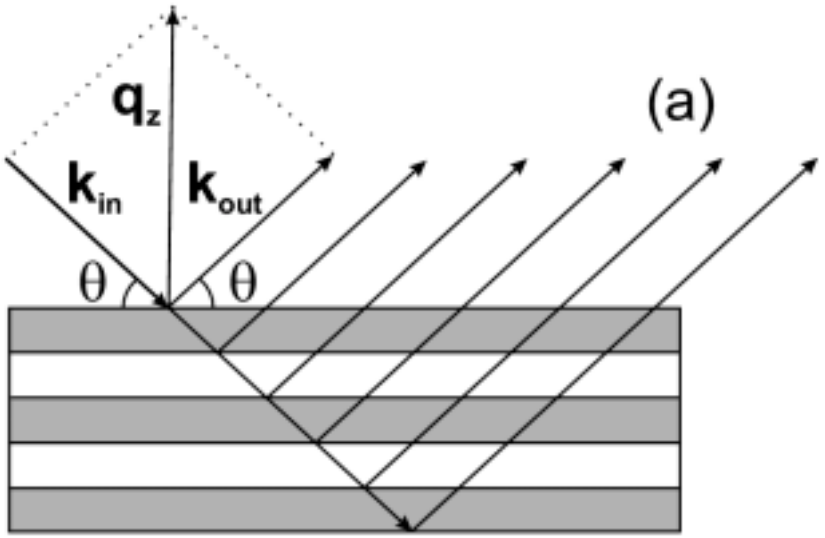

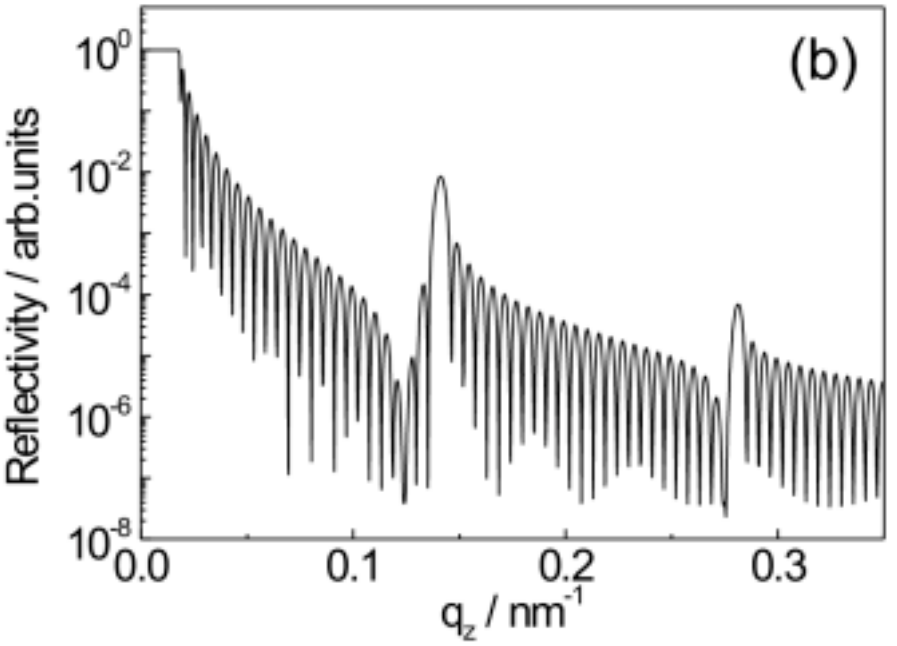

High-resolution rocking curve (8CB)

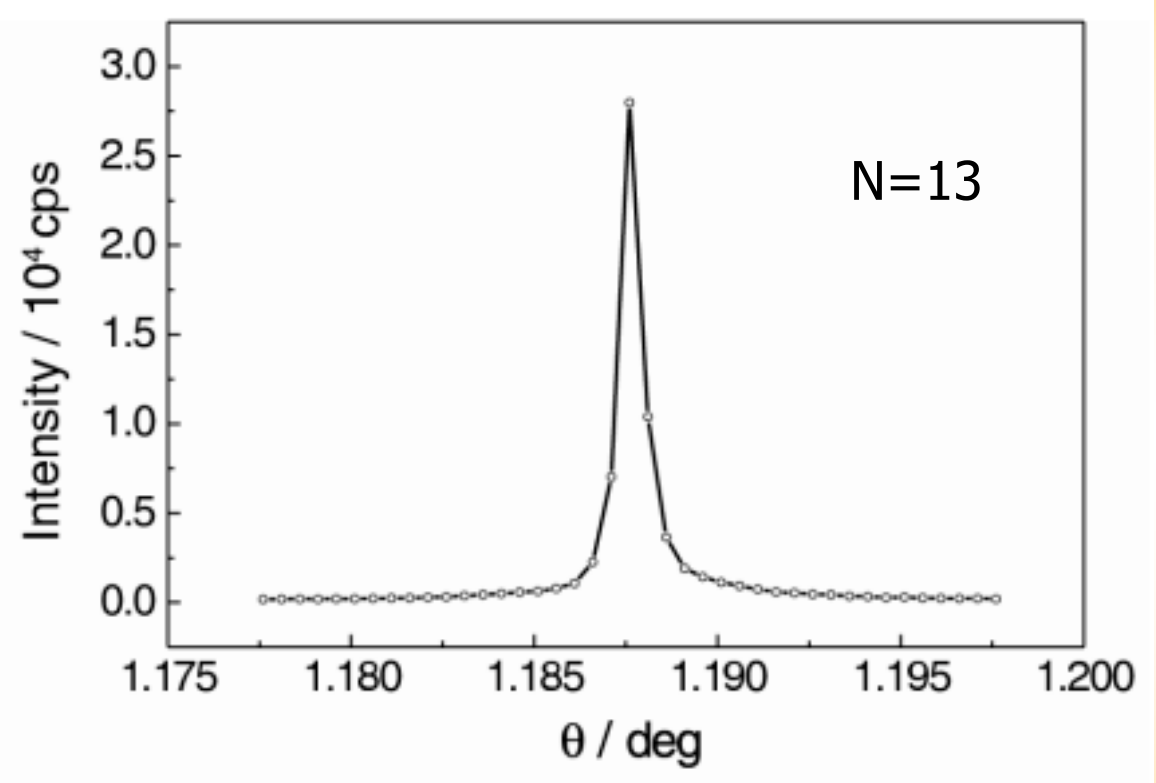

Bragg position reflectivity

Incoming beam:
pinhole 10 μm Ø

Detector slits: 30×30 μm^2

FWHM = 0.7 mdeg

Scattering setup

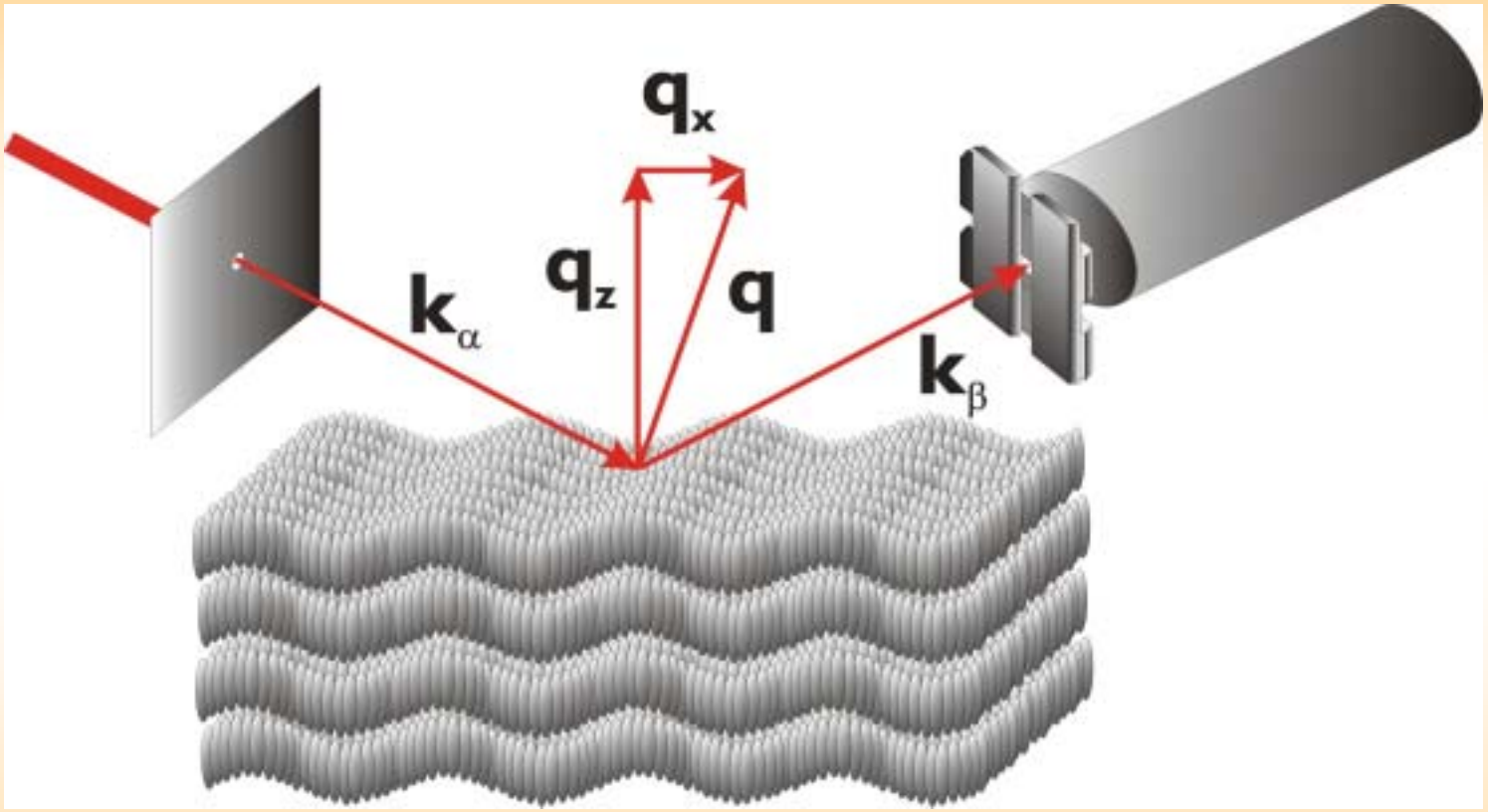

(x,y) plane || to the surface of the membrane

z ⊥ to the surface of the membrane

Setup parameters (Troika I, ESRF)

Third/fifth harmonic of set of three undulators.

Source size: 928×23 μm^2 ($s_H \times s_V$)

Mono: Si(111) at 8 or 13.4 keV

λ at 1.55 or 0.96 Å, $\Delta\lambda/\lambda \approx 10^{-4}$

Pinhole: 10 μm Ø at R = 44 m

Coherence lengths:

$\xi_{t,H} = \lambda R/(2s_H) \approx 8$ μm; $\xi_{t,V} \approx 300$ μm.

$\xi_l = \lambda/(\Delta\lambda/\lambda) \approx 1.6$ μm.

At the Bragg position $\theta \approx 1.5^o \rightarrow$
path length difference: $2L \sin\theta = 1.6$ μm $\rightarrow L_{max} \approx 30$ μm.

Detection system

Avalanche photo diodes

Perkin Elmer C30703.

Time resolution: ~ 0.7 ns (rise time).
Low background (thin, insensitive to high-energy photons).

A.Q.R. Baron, *Hyperfine Interactions* **125**, 29 (2000)

Correlators

FLEX01-8D — Correlator.com, small convenient box, lag time 8 ns.

Direct storage: store arrival times all individual pulses, calculate correlation function later.

Bunch structure of the storage ring at ESRF

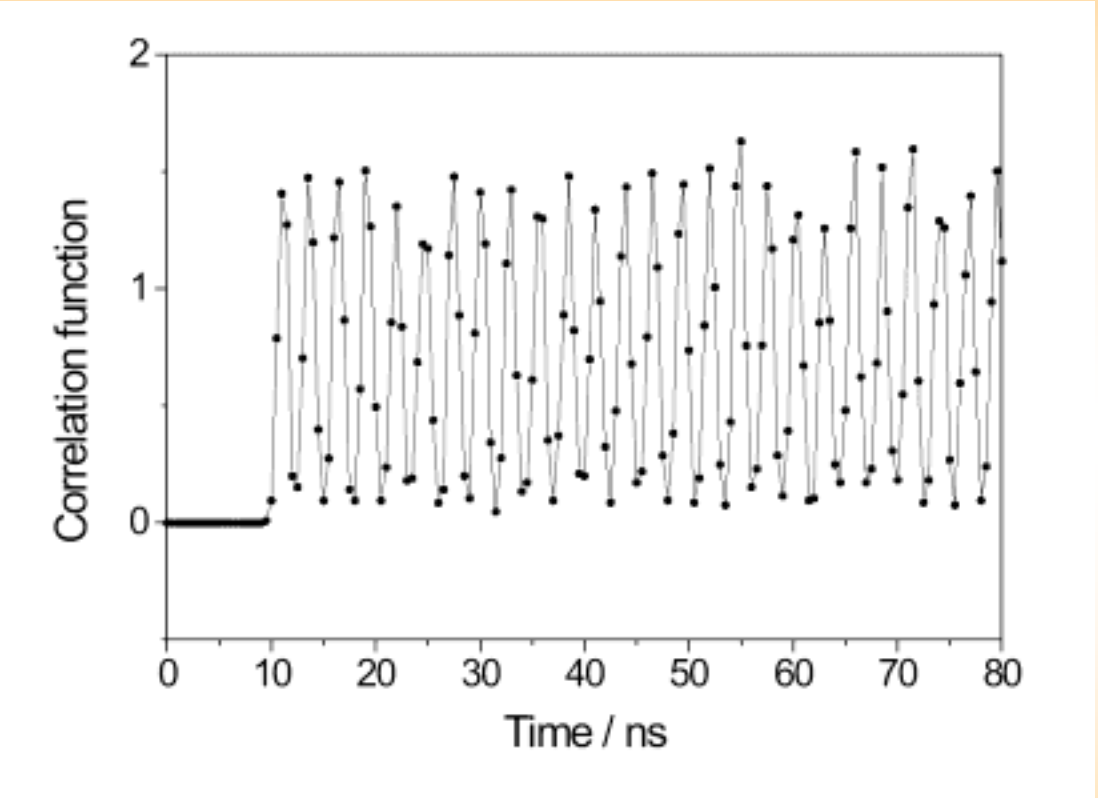

Continuous filling mode with 992 bunches equally spaced at 2.8 ns.
Rising edge of avalanche photodiode stored in memory of a
2 GHz computer board.

Landau-de Gennes-Hołyst Free Energy

$$F = \frac{1}{2}\int d^2 r_\perp \left\{ \int_{-L/2}^{L/2} dz\{B[\nabla_z u(x,y,z)]^2\} + K[\nabla_\perp^2 u(x,y,z)]^2\} + \right.$$
$$\left. \gamma\{[\nabla_\perp u(x,y,z=-L/2)]^2 + [\nabla_\perp u(x,y,z=L/2)]^2\} \right\}$$

Bend layers

$K \sim 10^{-11}$ N

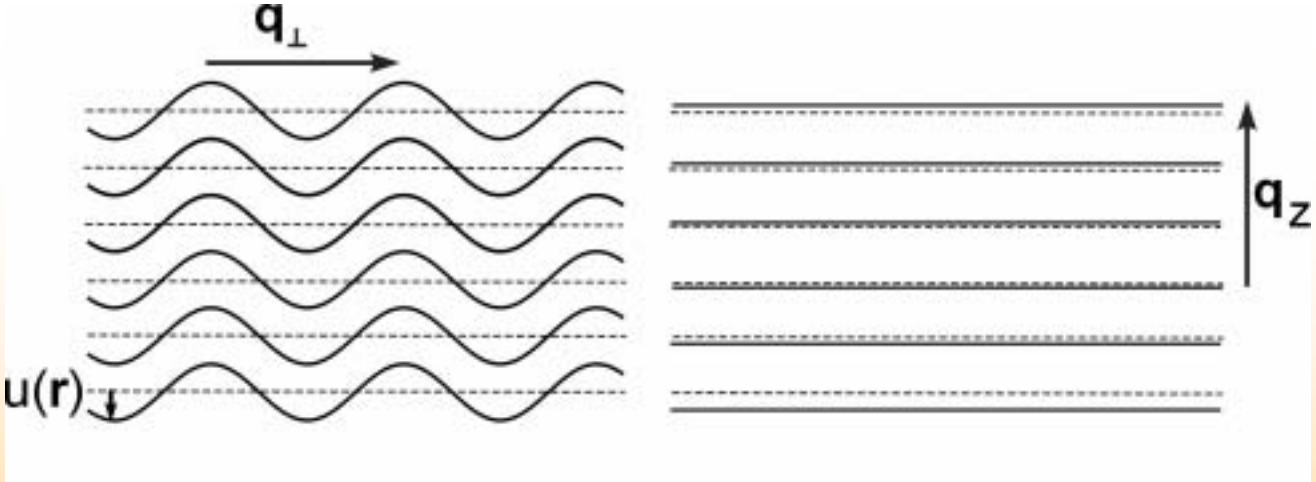

Compression layers

$B \sim 10^{7}$ N/m^2

$$\langle u^2(\mathbf{r})\rangle = \frac{k_B T}{8\pi\sqrt{KB}} \ln\left(\frac{L}{d}\right)$$

Fluctuations destroy layer ordering for large L

Relaxation regimes

$$\tau_{s,f} \approx \frac{2\rho_0}{\eta_3 q_\perp^2}\left(1 \mp \sqrt{1 - \frac{4\rho_0}{\eta_3^2 q_\perp^4}\left(Kq_\perp^4 + \frac{2\gamma}{L}q_\perp^2\right)}\right)^{-1}$$

transition at $q_{\perp,c} \approx \frac{2}{\eta_3}\sqrt{\frac{2\rho_0\gamma}{L}}$

$q < q_{\perp,c}$

Complex mode (oscillations):

$$\tau_s = \tau_f^*$$

$q > q_{\perp,c}$

$$\tau_s = \frac{\eta_3}{2\gamma/L + Kq_\perp^2}$$

$$\tau_s = \frac{\eta_3 L}{2\gamma}$$

$$\tau_s = \frac{\eta_3}{Kq_\perp^2}$$

A.N Shalaginov, D.E. Sullivan *Phys. Rev. E* **62** 699 (2000)

Dispersion curve

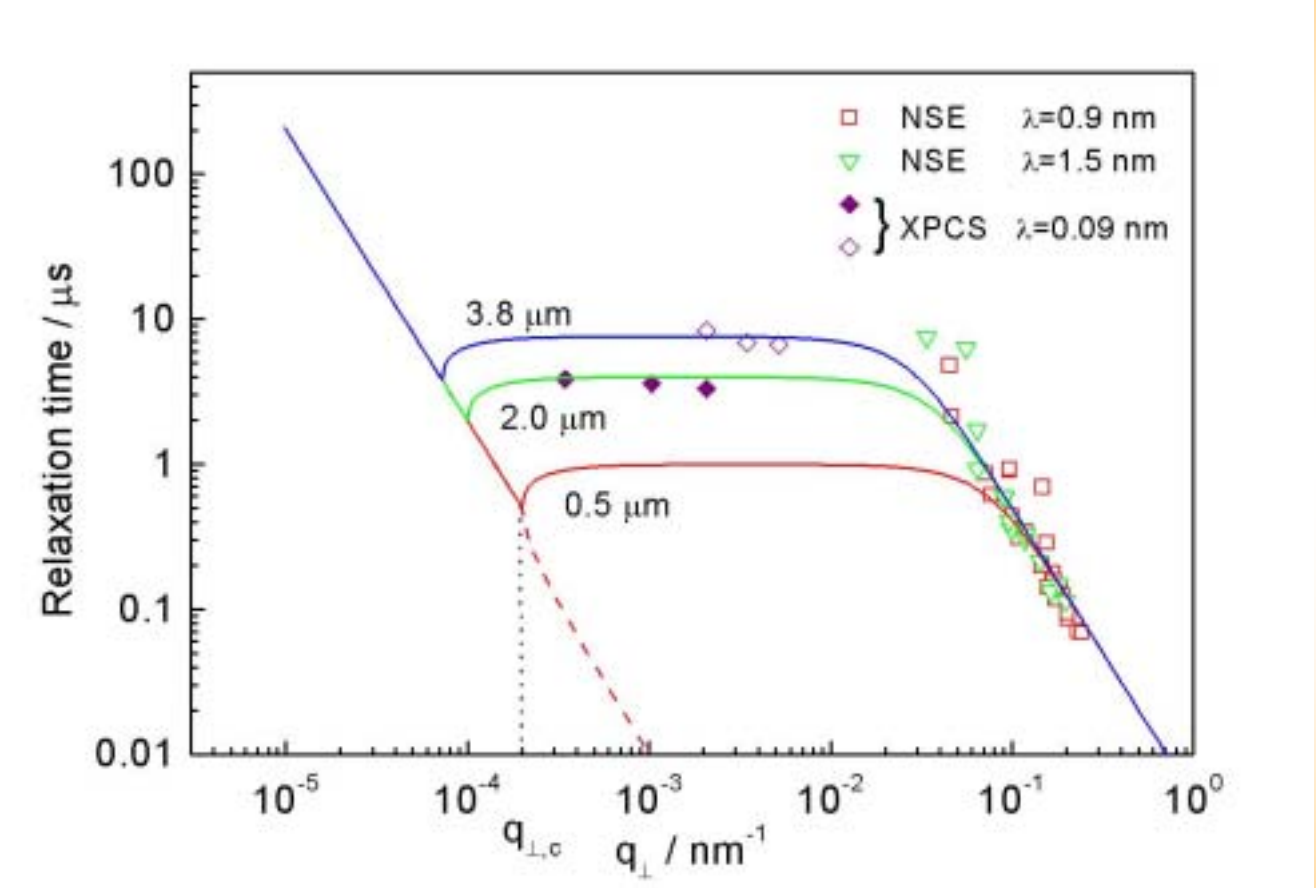

I. Sikharulidze, B. Farago, I. Dolbnya, A. Madsen, W. H. de Jeu,
Phys. Rev.Lett. **91** (2003) 165504

Off-specular Measurements (FPP)

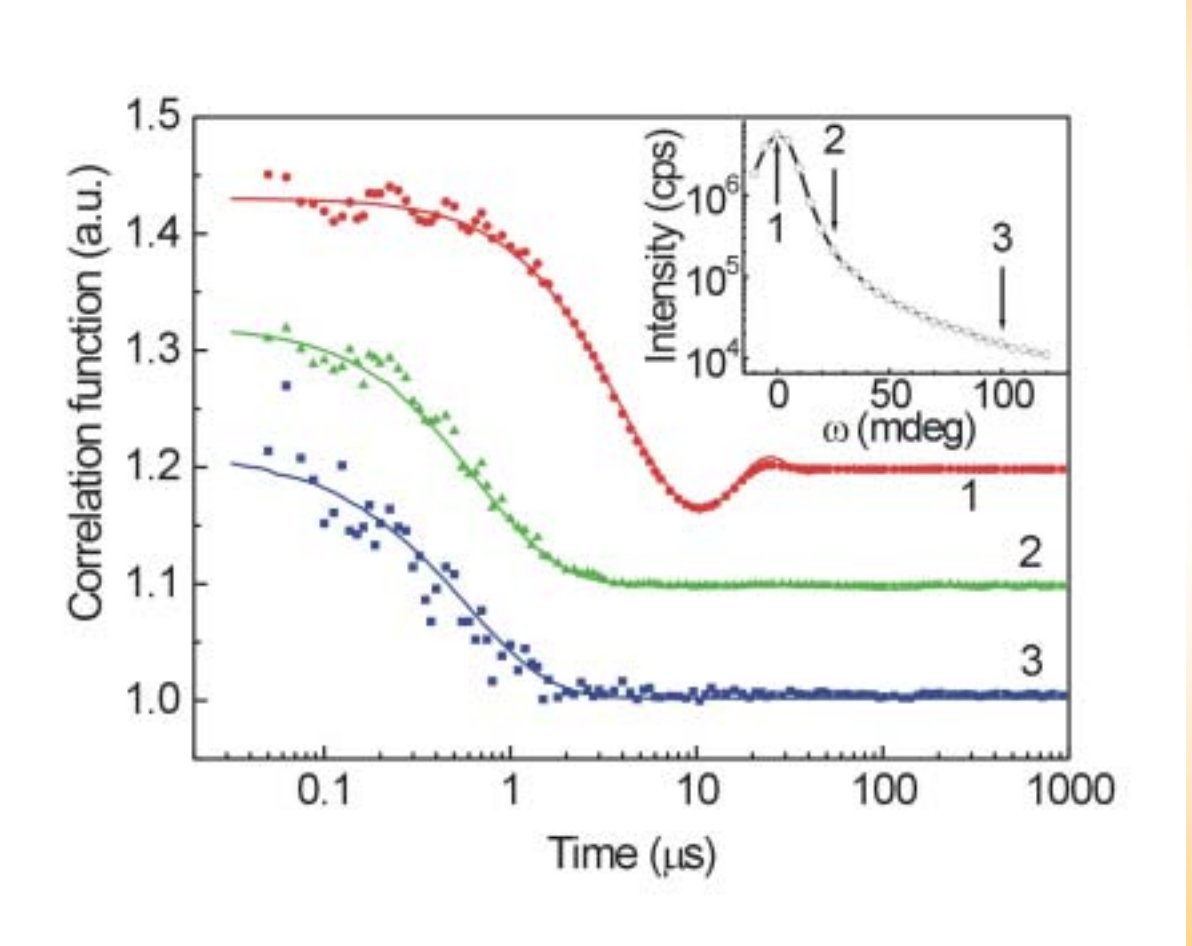

Neutron Spin Echo: Results (8CB)

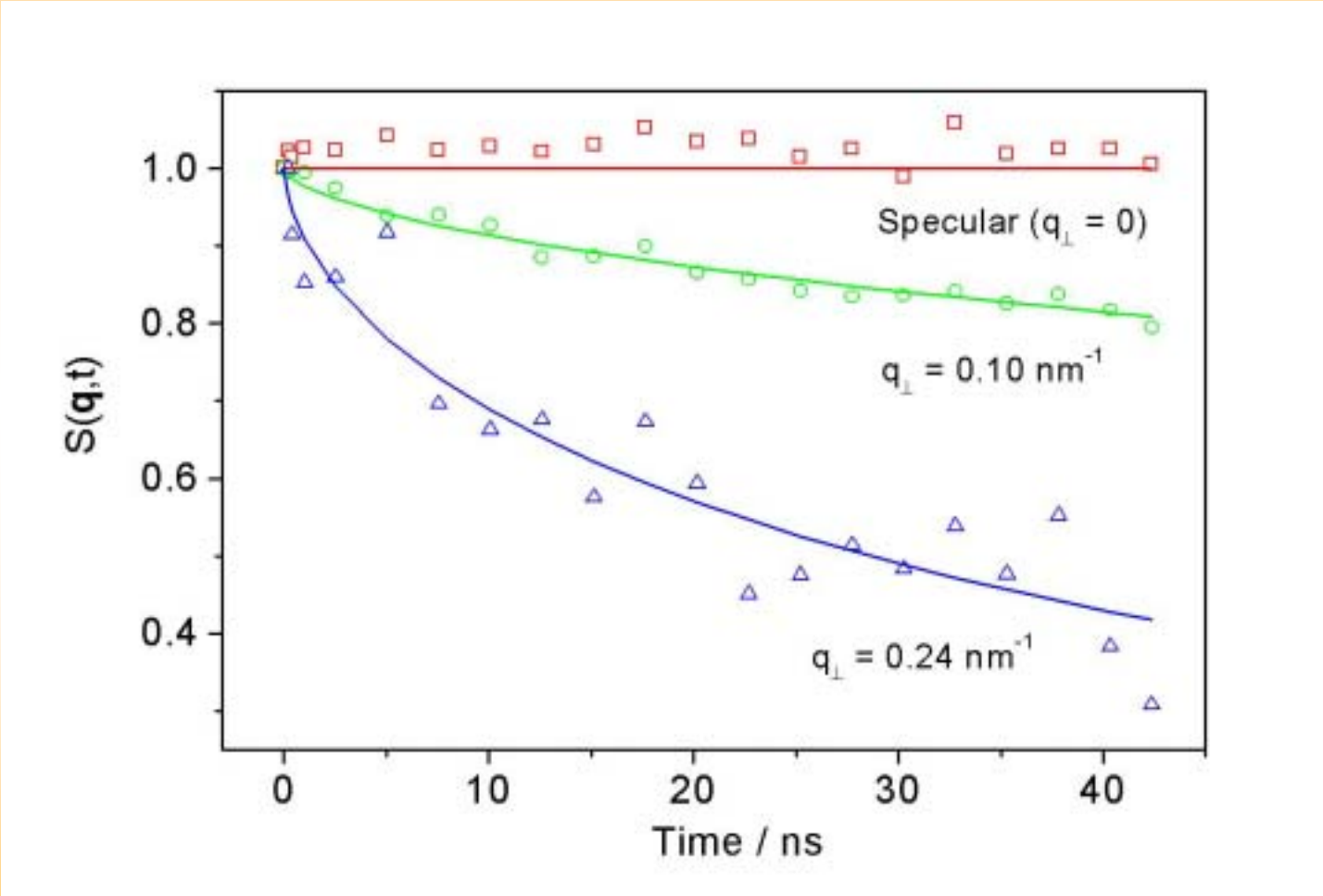

Homodyne-heterodyne detection

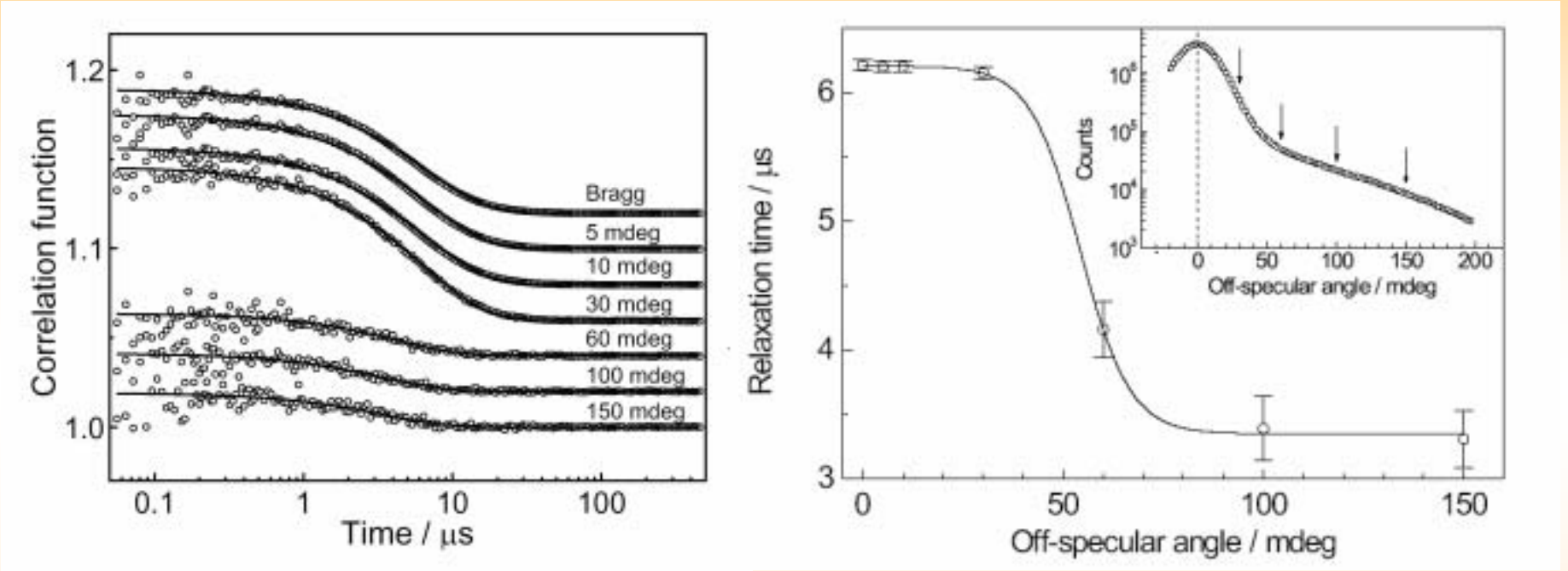

Off-specular: τ = 3.3 μs → homodyne detection.
Specular: τ = 6.2 μs → heterodyne detection.

Homodyne-heterodyne detection (2)

In presence of a reference signal:

$$E(t) = E_{\mathrm{ref}} + E_{\mathrm{s}}(t)$$

Substitution in $\langle I(t)I(t+\tau)\rangle$ leads to

$$\langle I(t)I(t+\tau)\rangle \approx I_{\mathrm{ref}}^2 + 2I_s I_{\mathrm{ref}} \mathrm{Re}[g_1(\tau)].$$

Dynamic light scattering:
Amplification of heterodyne signal by external grating.

Here in XPCS: Strong elastic Bragg peak acts as "internal" secondary source!

Dynamic Light Scattering

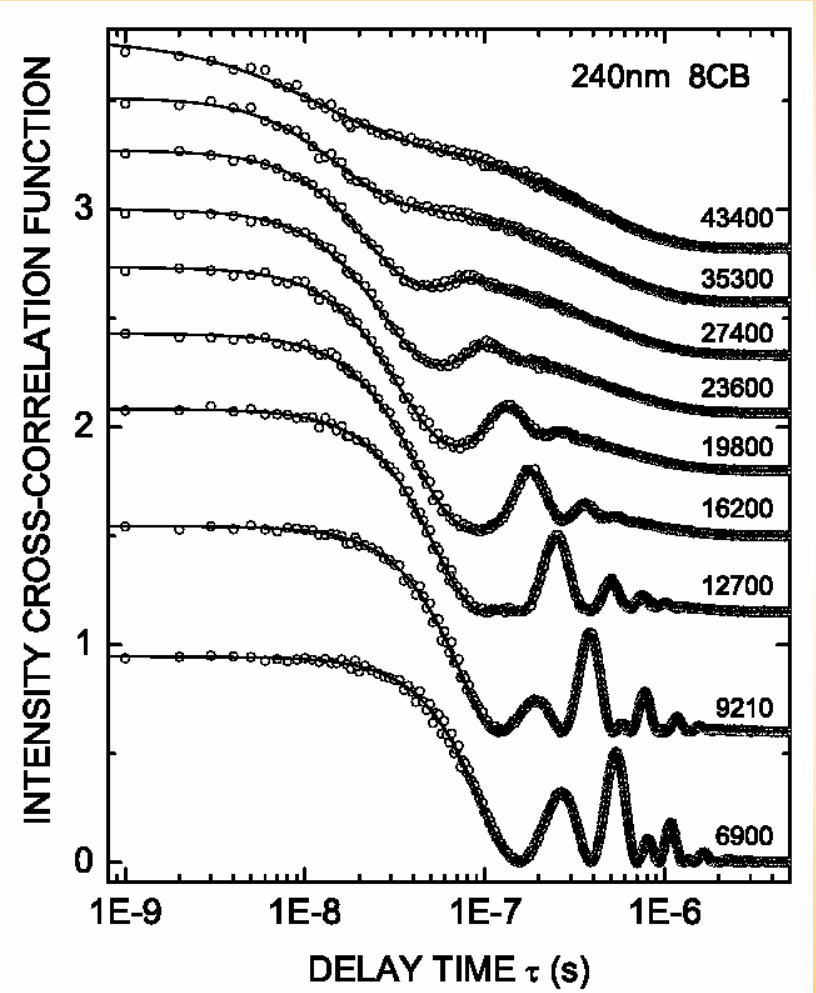

S. Sharma, K. Neupane, A. Adorjan,
A. R.Baldwin, and S. Sprunt
Phys. Rev.Lett. **94** (2005) 067801

Dispersion curve

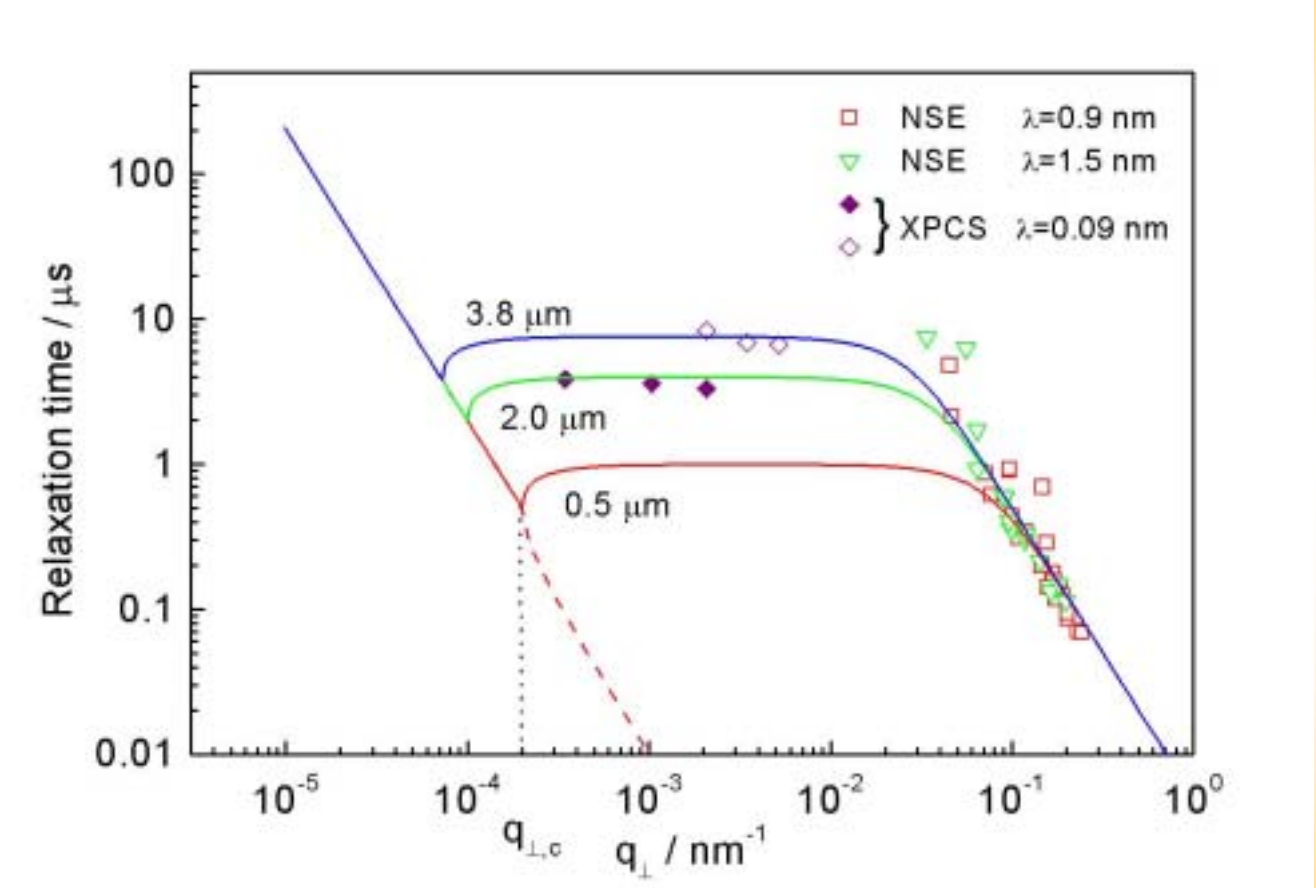

I. Sikharulidze, B. Farago, I. Dolbnya, A. Madsen, W. H. de Jeu,
Phys. Rev.Lett. **91** (2003) 165504

Thickness dependence (4O.8)

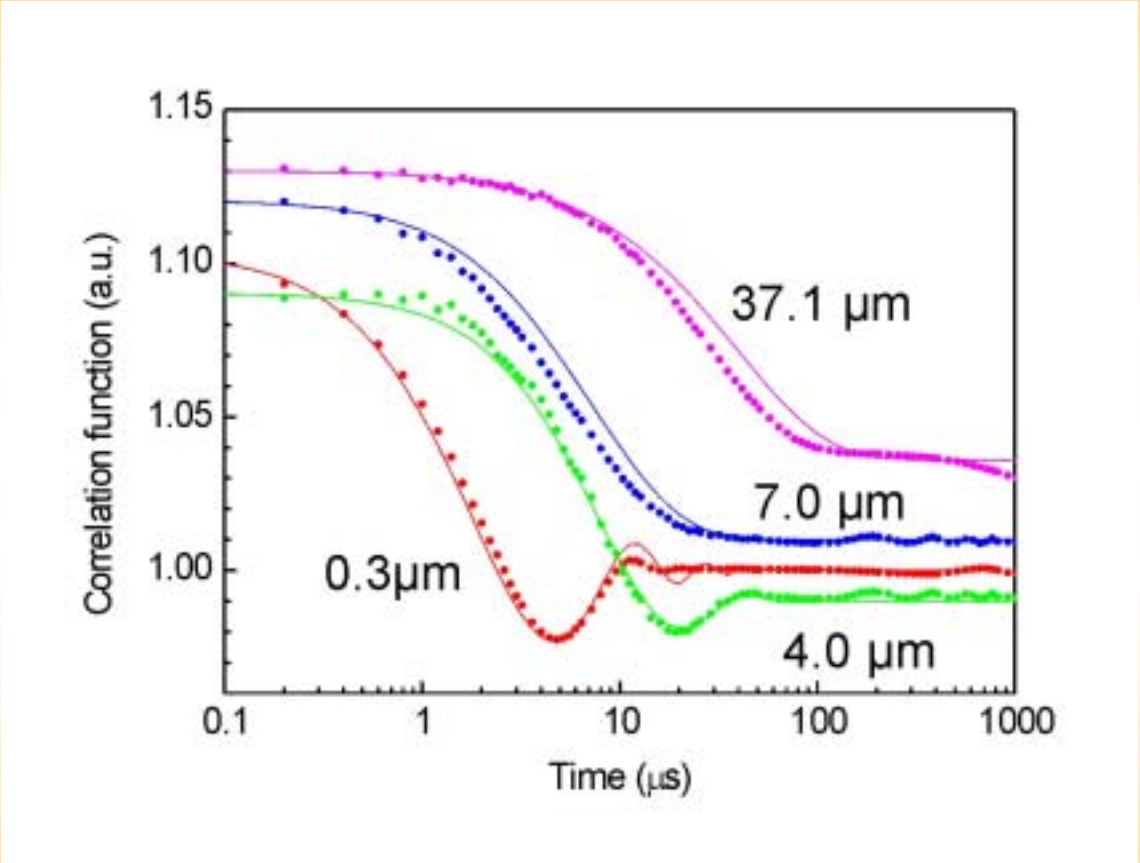

I. Sikharulidze, I.P. Dolbnya, A. Fera, A. Madsen, B.I. Ostrovskii,W.H. de Jeu, Phys. Rev. Lett. **88**, 115503 (2002)

Scattering angle dependence

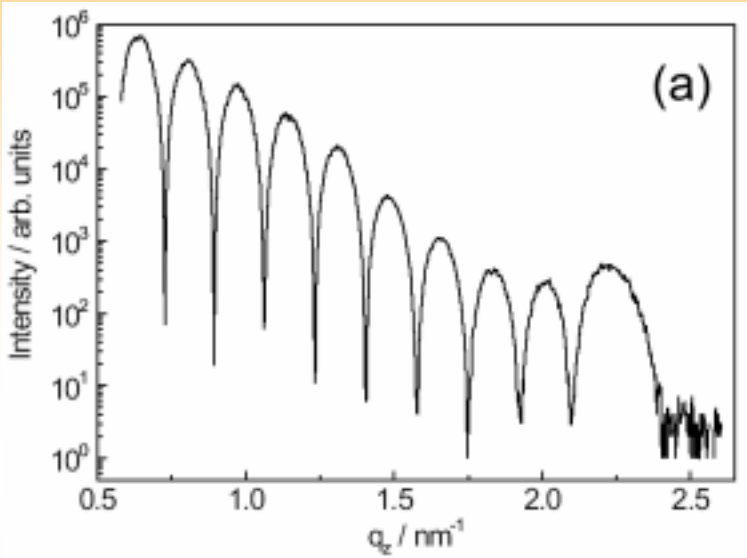

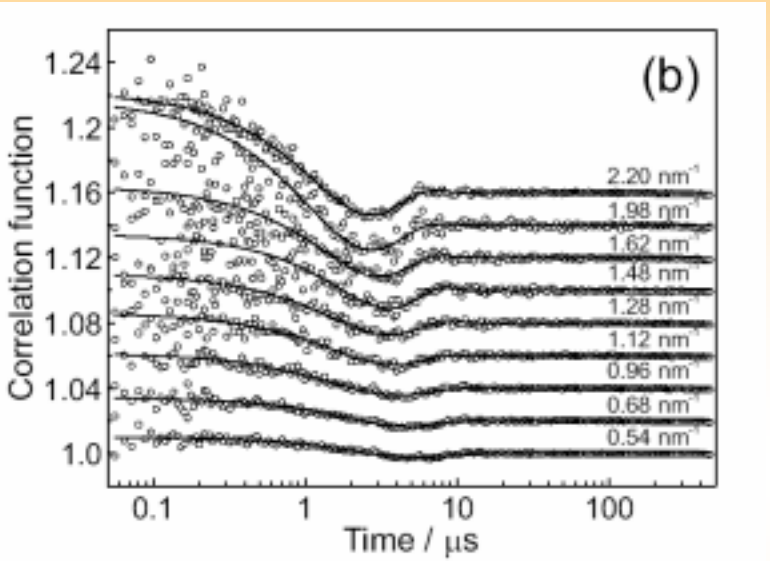

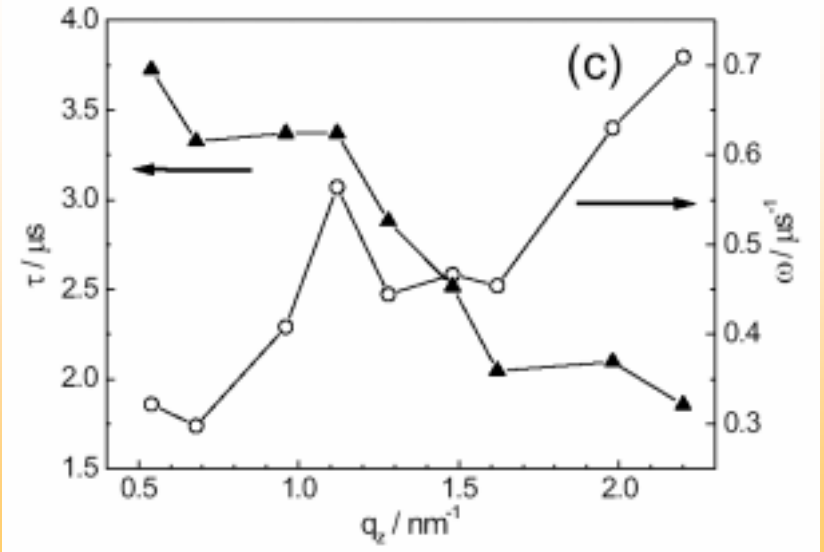

Coherence volume decreases with increasing scattering angle giving faster relaxations.

I. Sikharulidze, I.P. Dolbnya, A. Madsen, W.H. de Jeu, Opt. Commun. **247**, 111 (2005)

Perfect membrane puzzle

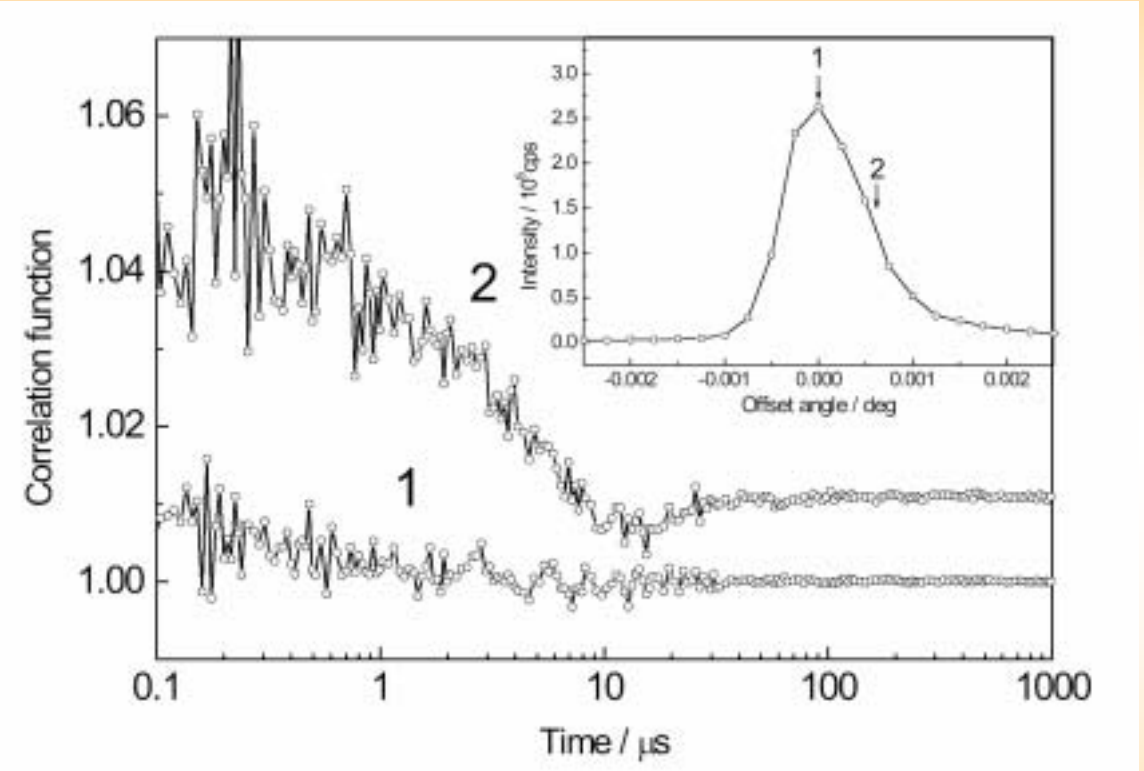

In perfectly ordered membranes contrast at the Bragg disappears

Model

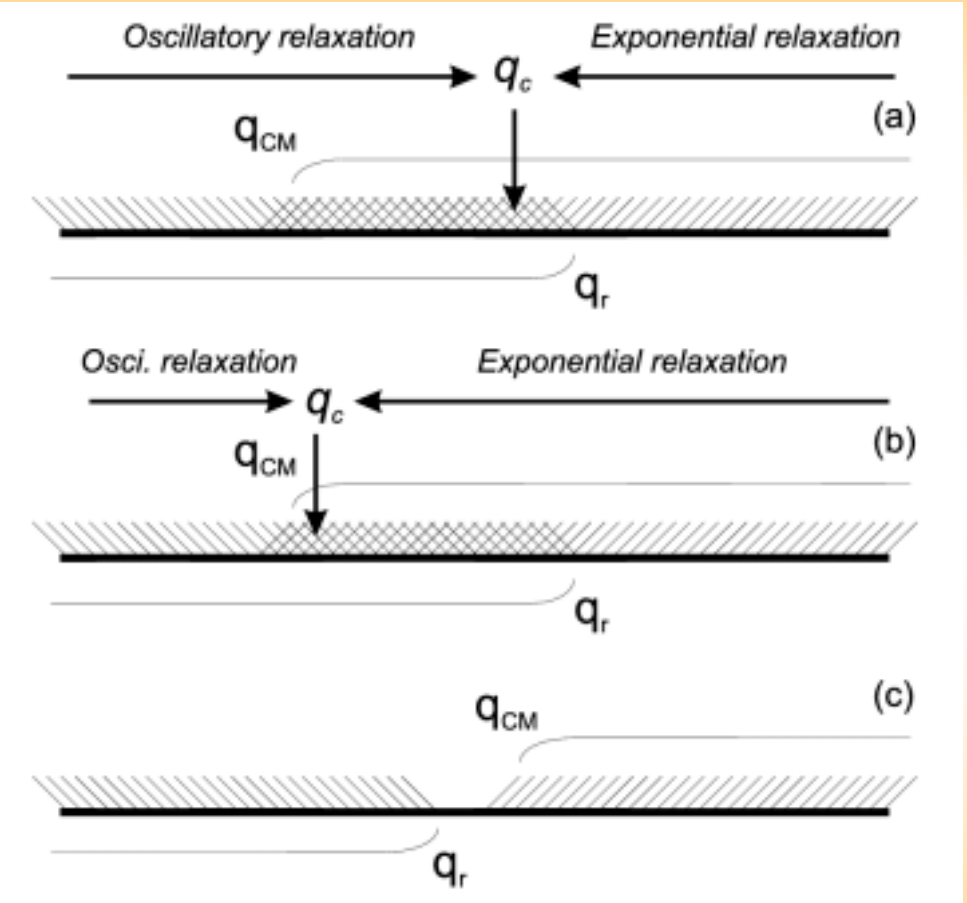

Oscillations

Exponential relaxation

Zero contrast

I. Sikharulidze and W.H. de Jeu, Phys. Rev. E (in press)

Mosaic vs. Cross-over Wavevector

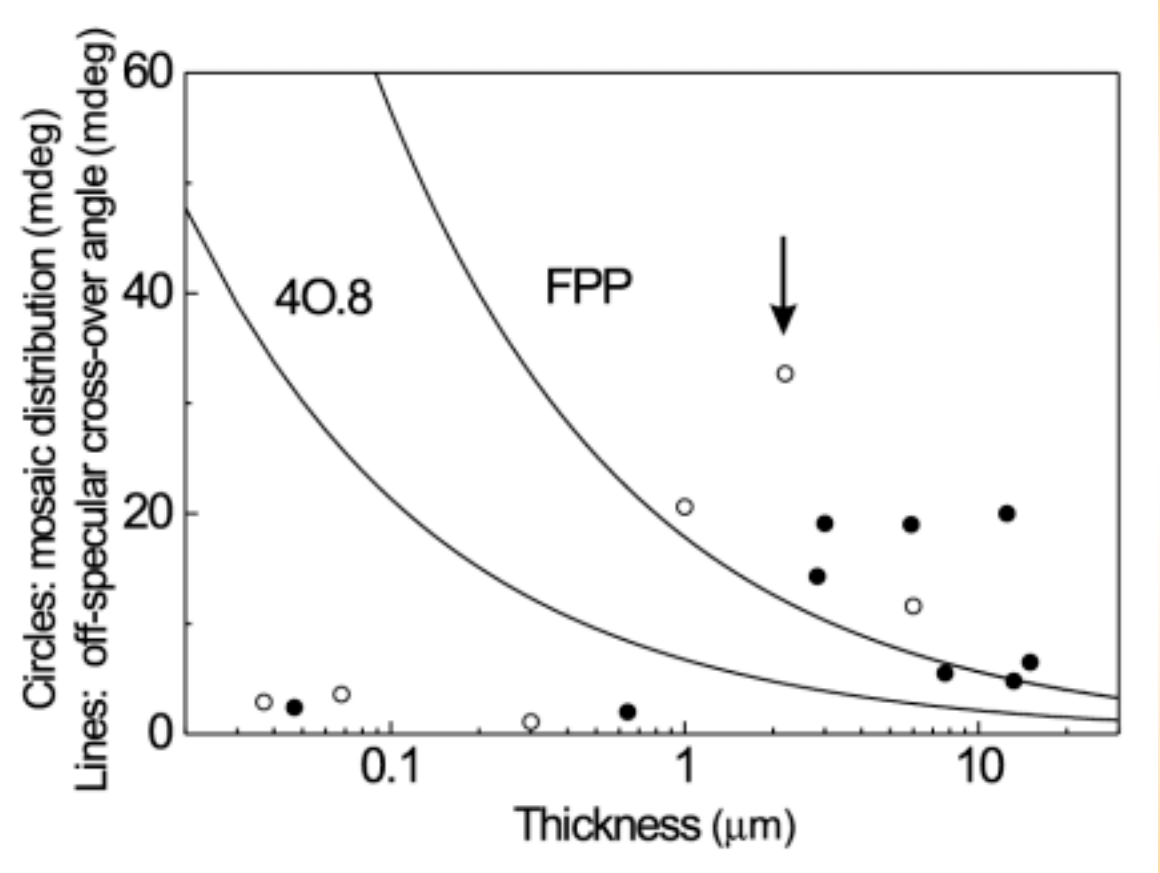

- o 4O.8
- ● FPP

Chellenge: Coherence induced oscillations

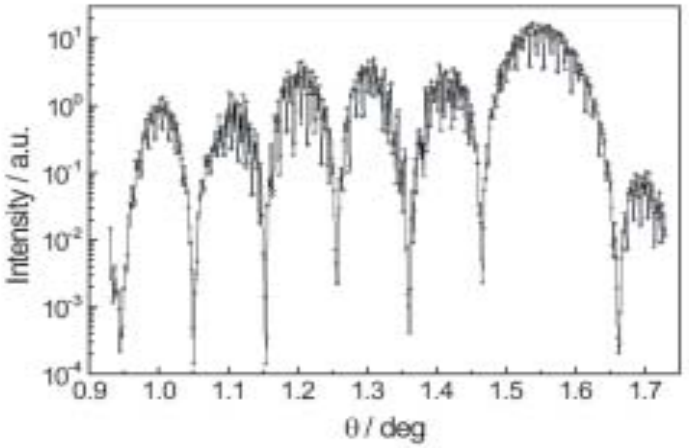

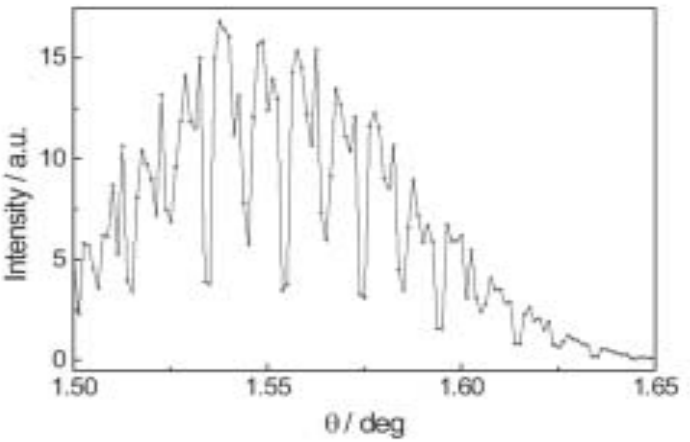

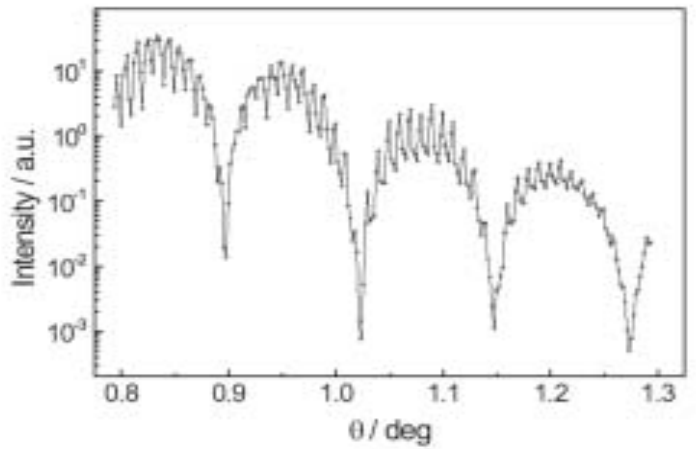

Two slit interference type oscillations on the top of smectic membrane reflectivity curve

Chellenge: Coherence induced oscillations (2)

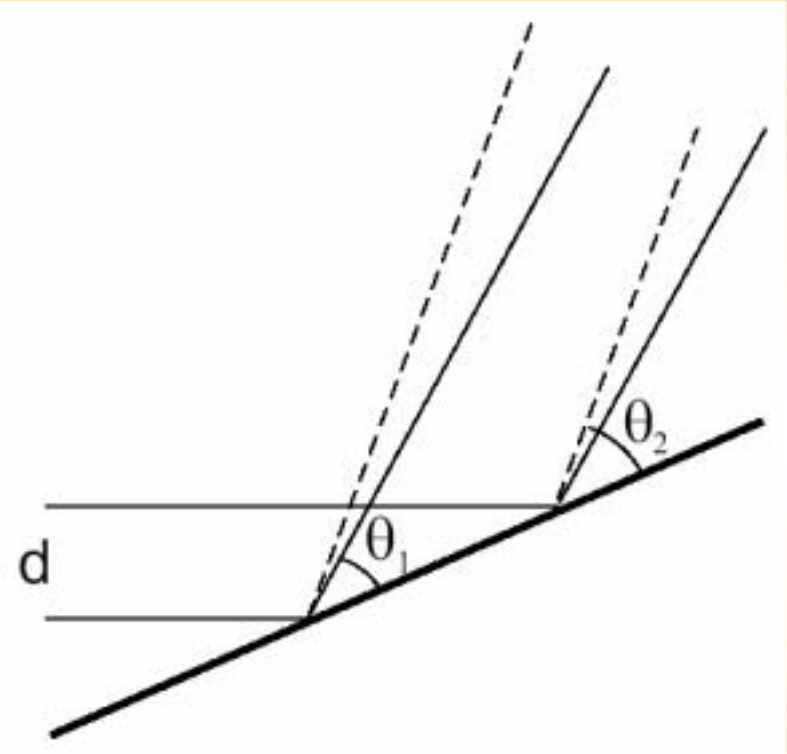

$$\theta = (\theta_1 + \theta_2)/2 = 1.544^\circ$$

$$\Delta\theta = \theta_1 - \theta_2 = 0.02^\circ$$

$$\lambda = 0.154 \text{ nm}$$

$$d \simeq 0.4\ \mu\text{m}$$

$$d = \frac{\lambda}{2(\cos\theta_1 - \cos\theta_2)} \sin(\theta) = \frac{\lambda}{4\sin(\Delta\theta/2)\sin(\theta/2)} \sin(\theta) \approx \frac{\lambda}{\Delta\theta}$$

Conclusions

- Mosaicity of the sample and coherence volume define a wave vector "window" of fluctuations detected in specular XPCS measurements.
- If the cross-over wave vector is close to the lower edge of the "window" exponential relaxation is observed and if it is close to higher edge - oscillatory relaxations.
- In case of the highly uniform samples with narrow mosaic "window" is empty, which results in the absence of contrast in XPCS
- A q_z-dependence is observed which parallels the projected coherence length (footprint).
- Both heterodyne (at the specular ridge) and homodyne (off-specular) detection schemes have been realized.